DOI: 10.1007/s12541-010-0081-5

Vibro-Acoustic Characteristics of An Annular Disk with Narrow Radial Slots

Hyeongill Lee[1,#]

1 School of Mechanical and Automotive Engineering, Kyungpook National University, 386, Gajang-dong, Sanju, Kyungbook, South Korea, 742-711
Corresponding Author / E-mail: hilee@knu.ac.kr, TEL: +82-54-530-1406, FAX: +82-54-530-1407

KEYWORDS: Sound radiation, Annular disk, Eigensolution, Radial slot, Flexural mode, Acoustic power

Analytical solutions for vibro-acoustic characteristics of a thin annular disk containing narrow radial slots have been proposed with numerical and limited experimental verifications. Structural characteristics of split and repeated modes of the disk are expressed in terms of eigensolutions for the corresponding uniform disk that has same geometric configuration. Sound radiations due to the modal vibrations are calculated using pre-developed analytical solution based on the structural data obtained above. Structural and acoustic responses of the disk for a stationary concentrated harmonic force have been studied using the modal expansion technique. Based on these results, the effects of relative location of the excitation to the slots on the vibro-acoustic responses as well as interactions between sound radiations for two split modes are investigated. The results demonstrate that the introduced procedure has reasonable accuracy obtaining vibro-acoustic characteristics of a thin annular disk containing narrow radial slots.

Manuscript received: March 25, 2009 / Accepted: July 21, 2010

NOMENCLATURE

P = far field sound pressure (Pa)
$\mathbf{r}_f$ = position vector for the excitation
$\mathbf{r}_p$ = position vector for the acoustic responses
$\mathbf{r}_s$ = position vector for the structural responses
R = radius for far-field location (m)
S_s= surface of source (radiator)
S_v= surface of control volume
W = radial dependent transverse displacement (m)
Φ = flexural mode shape of the uniform disk
Γ = modal sound radiation of the uniform disk
Λ = modal sound radiation of the disk containing radial slots
Π = acoustic power from the disk vibration (W)
Ψ = flexural mode shape of the disk containing radial slots
ϕ = azimuthal angle for far-field location (rad)
η = structural modal participation factor
θ = cone angle for far-field location (rad)

1. Introduction

Structural vibration and sound radiation due to the vibration have been studied by many researchers so far.[1-15] Also, out-of-plane (flexural) vibration is a major source of sound radiation from many mechanical, electrical or structural components having annular or circular disk shape. In many cases, intentional or unavoidable asymmetries in the geometry are introduced and these asymmetries substantially alter the vibration of plates along with sound radiation due to the vibration. This study focuses on the vibro-acoustic characteristics of the thin annular disk containing narrow radial slots. If acoustic characteristics of asymmetric disk were clearly defined, unavoidable asymmetries, such as crack, in the annular or circular components could be easily detected by acoustic test only. Further, effective locations for the excitation(s) and response(s) for this test can be easily determined based on the characteristics.

Structural eigensolutions for the out-of-plane modes of the disk with free-free boundary condition have been calculated with perturbation method based on the thin plate theories. The results are examined with numerical analysis and experiments. Sound radiations due to the modal vibrations have been calculated using pre-developed analytical solution and also verified with a numerical method. Based on the results, acoustic responses for a harmonic excitation are obtained using the modal expansion technique. In addition, the same problem has been solved numerically using boundary element method to confirm analytical solution. Finally, interaction between the sound radiations from two split vibration

modes is investigated and an analytical formulation for sound powers is proposed.

There are many articles on the structural dynamics of circular or annular disk containing radial slots.[1-6] Mote[1] investigated stability of annular disk having radial slots using finite element method. Yu and Mote[2] claimed that radial slots introduce geometric asymmetry that splits some, vibration modes but not all. Honda et al.[3] investigated structural response of asymmetric circular disk to a concentrated harmonic force moving around the disk using mode expansion procedure. Shen and Mote[4] examined the vibration of circular plates with evenly spaced radial inclusions that split some of the repeated vibration modes and expressed the eigenfunctions of repeated modes of asymmetric disk as superposition of a subset of the uniform disk. Rim and Mote[5] studied unstable phenomenon (kick-off) of a circular saws having radial slots with stability analyses based on finite element method, experiments and numerical analyses. Lee[6] investigated modal vibration of annular disks containing narrow radial slots and claimed that vibration modes as well as natural frequencies are affected by the slots when the slot length is above a certain limit and perturbation method proposed by Yu and Mote can not precisely predict eigensolutions of the disks with slots.

Sound radiations from annular disks containing radial slots have not been adequately examined though limited acoustic studies have considered either flexural vibration modes or rigid body piston motions of thin disks.[7-13] For instance, Thompson[7] computed self and mutual radiation impedances of a uniformly vibrating annular or circular piston by integrating of the far-field directivity function. Lee and Singh[8] proposed a polynomial approximation for modal acoustic power radiation from a thin annular disk using the far-field sound pressure and radiation impedance approach. Levine and Leppington[9] developed an analytical solution for active and reactive powers from a planar annular membrane given axisymmetric motions. Rdzanek and Engel[10] suggested asymptotic formulas for power from a thin annular disk with clamped edges. Wodtke and Lamancusa[11] investigated a circular plate using finite element analysis and then calculated the radiation via the Rayleigh integral formula. Finally, Lee and Singh[13] expressed acoustic powers from vibrating annular disks as the linear combinations of self and mutual radiation powers. However, none of these studies has examined radiation from an annular disk with radial slots.

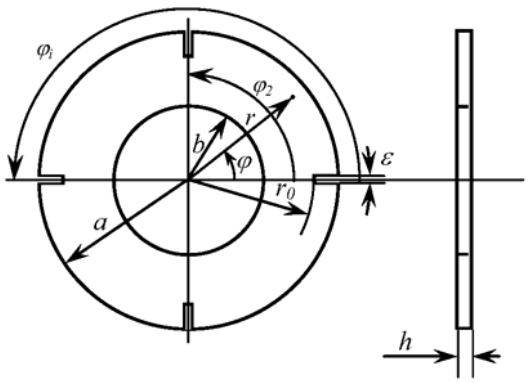

Fig. 1 Annular disk containing 4 identical narrow radial slots

Fig. 1 illustrates the example disc with 4 identical narrow radial slots. The disc is assumed to be stationary with free-free boundaries and made of an undamped, isotropic material. Also, Table 1 provides geometric dimensions and material properties of the sample disc.

Table 1 Disk dimensions and material properties

Outer Radius	a	139.0 mm
Inner Radius	b	82.5 mm
Thickness	h	3.2 mm
Slot Length Ratio	$\alpha = (a-r_0)/(a-b)$	0.09 / 0.45
Slot Sector Angle	ε	1.1°
Mass Density	ρ_d	7905.9 kg/m^3
Young's Ratio	E	205 GPa
Poisson's Ratio	ν	0.295
Plate Stiffness	D_b	611.2 Nm

Primary assumptions are as follows: (1) Structural and acoustic systems are linear time-invariant. (2) The complicating effects such as fluid loading and acoustic scattering from the disc edges are negligible. (3) Free and far field sound pressure at an observation point (r_p) is generated by only the vibratory motions at the normal surfaces and inner or outer radial surfaces do not contribute to total far-field sound pressure. Chief objectives of this article are as follows. (1) Examine the effects of narrow radial slots on the vibro-acoustics of an annular disk. (2) Suggest semi-analytical solutions for sound radiation due to modal vibration of annular disks with radial slots. (3) Investigate the interactions between sound radiations from any two split modes.

2. Modal Characteristics

2.1 Structural Characteristics

The equation of motion and vibration modes for the flexural vibration of a uniform annular disk can be expressed as follows.[2]

$$\left(\frac{\partial^2}{\partial r^2} + \frac{1}{r}\frac{\partial}{\partial r} + \frac{1}{r^2}\frac{\partial^2}{\partial \varphi^2} \right)^2 w - \lambda^4 w = 0 \tag{1}$$

$$\begin{aligned} w_{mn}(r,\varphi) &= W(r)\cos n(\varphi) \\ W(r) &= C_1 J_n(\lambda_{mn} r) + C_2 Y_n(\lambda_{mn} r) + C_3 I_n(\lambda_{mn} r) + C_4 K_n(\lambda_{mn} r) \end{aligned} \tag{2}$$

Here, λ is non-dimensionalized eigenvalue, and w is displacement of transverse vibration, J_n and Y_n are the Bessel functions of first and second kinds and I_n and K_n are modified Bessel functions of first and second kinds. Also, n is the order of the Bessel function representing the number of nodal diameters and m is the order of eigenvalues representing the number of nodal circles. In addition, for the free-free disk, boundary conditions at inner and outer edges can be expressed as follows:

$$\begin{aligned} &\frac{\partial^2 w}{\partial r^2} + \nu\left(\frac{1}{r}\frac{\partial w}{\partial r} + \frac{1}{r^2}\frac{\partial^2 w}{\partial \varphi^2} \right) = 0 \\ &\frac{\partial}{\partial r}\left(\frac{\partial^2 w}{\partial r^2} + \frac{1}{r}\frac{\partial w}{\partial r} + \frac{1}{r^2}\frac{\partial^2 w}{\partial \varphi^2} \right) + \frac{(1-\nu^2)}{r^2}\frac{\partial^2 w}{\partial \varphi^2}\left(\frac{\partial w}{\partial r} + \frac{1}{r}\frac{\partial w}{\partial \varphi} \right) = 0 \end{aligned} \tag{3}$$

Eigenvalues and corresponding mode shapes of a uniform annular disk can be determined from Eq. (1) and (2). In this case, all the modes having more than one nodal diameter have repeated natural frequencies.

According to the previous studies, radial slots introduced in the disk split some, but not all, repeated natural frequencies into two distinct values. Natural frequency parameters for an annular disk containing narrow radial slots given in Fig. 1 can be approximated using natural frequencies and vibration modes of the uniform disk without any radial slot as Eq. (4).[2]

$$\lambda_{mn} = (\lambda_u)_{mn} + \varepsilon(\lambda_1)_{mn} + O(\varepsilon^2)$$

$$(\lambda_1)_{mn} = \frac{(\lambda_u)_{mn}\sum_{i=1}^{4}\int_{r_0}^{b}(w_u)_{mn}(r,\varphi_i)rdr - \sum_{i=1}^{4}\int_{r_0}^{b}P\left((w_u)_{mn}(r,\varphi_i)\right)rdr}{\int_{r_0}^{r}(w_u)_{mn}^2 dr}$$

$$P(w) = \left(\nabla^2 w\right)^2 + 2(1-\nu)\left[\begin{array}{l}\left(\frac{1}{r}\frac{\partial^2 w}{\partial r\partial\varphi} + \frac{1}{r^2}\frac{\partial w}{\partial\varphi}\right) \\ + \frac{\partial^2 w}{\partial r^2}\left(\frac{1}{r}\frac{\partial w}{\partial r} + \frac{1}{r}\frac{\partial^2 w}{\partial\varphi^2}\right)\end{array}\right] \quad (4)$$

$$\nabla^2 = \frac{\partial^2}{\partial r^2} + \frac{1}{r}\frac{\partial}{\partial r} + \frac{1}{r^2}\frac{\partial^2}{\partial\varphi^2}$$

Here, λ_{mn} is natural frequency parameter for mode (m, n) of disk with slots, $(\lambda_u)_{mn}$ is natural frequency parameter for the same mode of the uniform disk, $(w_u)_{mn}$ is the corresponding vibration mode, ε is a uniform sector angle for each slot, ∇^2 is bi-harmonic operator. Also, it was claimed that the vibration mode corresponding to one of the split eigenvalues has its nodal line on the slots and mode for the other natural frequency has its anti-nodal line on the slots. Consequently, vibration modes for the two split eigenvalues can be expressed as follows assuming no changes in the w(r) with the inclusion of slots.[2]

$$\psi_{mn,c}(r,\varphi) = W(r)\cos n(\varphi) + O(\varepsilon)$$
$$\psi_{mn,s}(r,\varphi) = W(r)\sin n(\varphi) + O(\varepsilon) \quad (5)$$

Here, c means the split mode that has anti-nodal line on the slot and s means the split mode that has nodal line on the slot.

Eigenvalues for two sample disks are obtained using Eq. (4) and compared with numerical data along with those of uniform disk without any slot. First, non-dimensional eigenvalues for selected modes of three disks with free-free boundaries are compared with finite element data in Table 2. In the finite element method, first 9 out-of-plane modes have been identified with a model that includes 2104 solid brick elements and 4512 nodes.[16] As one can see in the table, the differences between data sets from two approaches increase with α. Only when α < 0.09, the differences between two set are less than 1.0% and Eq. (3) and (4) can be used to obtain eigenvalues of disks with slots. Recently, the author[6] investigated above approach explained in Eq. (4) and (5). According to the result, modal strain energy distributions are globally affected by the introduced radial slots contrary to the basic assumption for Eq. (4) and (5) when α = 0.45.[6] Consequently, these variations should be taken into account to get correct eigenvalues which are very close to the numerical values in Table 2. So, when α = 0.45, the numerical values will be used in further investigations in this study.

Table 2 Eigenvalues for the sample disks with free-free boundary condition

Mode Indices			Non-dimensional Eigenvalues ($\lambda^2 = \omega_n a^2(\rho_d h/D_b)^{1/2}$)					
			α = 0.09		α = 0.45		α = 0	
m	n	q	Analytical	Numerical	Analytical	Numerical	Analytical	Numerical
0	2	c	3.95	3.93	3.94	3.71	3.96	3.93
0	2	s	3.96	3.93	3.96	3.80		
0	3	-	10.79	10.70	10.79	10.10	10.79	10.72
0	4	c	20.20	20.03	20.16	18.74	20.24	20.30
0	4	s	20.24	20.04	20.26	18.80		

Modal displacements in the disk with slots were also investigated revealing that the effects of slots on the mode shapes depend on mode types.[6] For example, $\Psi_{02,c}$, $\Psi_{02,s}$ and $\Psi_{04,s}$ have only small distortions in the limited areas and can be approximated by Φ_{02} and Φ_{04}.

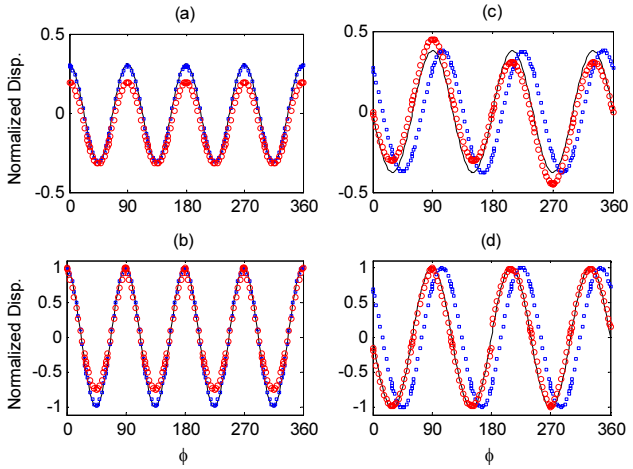

Fig. 2 Normalized modal displacement. (a) $\Psi_{04,c}$ inner (b) $\Psi_{04,c}$ outer (c) Ψ_{03} inner (d) Ψ_{03} outer. Key: ——, α = 0.0; ▫ ▫ ▫, α = 0.09; ◦ ◦ ◦, α = 0.45

On the other hand, Ψ_{03} and $\Psi_{04,c}$ include global shifts and can not be appropriately represented by Φ_{03} or Φ_{04} when α is above a certain limit.[6] Modal displacements at inner and outer edges in $\Psi_{04,c}$ and Ψ_{03} are compared in Fig. 2. As one can see in the figure, the displacement at inner and outer edge for $\Psi_{04,c}$ globally shift in opposite direction and those for Ψ_{03} shift in same direction. In both cases, the amount of shifts are proportional to α and when α = 0.09, $\Psi_{04,c}$ and Ψ_{03} are almost same as Φ_{04} and Φ_{03} respectively.

According to the previous studies,[4,6] $\Psi_{mn,q}$ can be approximated as a linear combination of Φ_{mn}s. Here, q is the split index used in Eq. (5). Same approach is used for Ψ_{03} and $\Psi_{04,c}$ with α = 0.45 where the two modes can not be reasonably approximated with Φ_{03} or Φ_{04} only. The expansions for two modes can be expressed following equation.

$$\Psi_{03}(r,\varphi) \cong 1.02\Phi_{03} - 0.032\Phi_{11}$$
$$\Psi_{04,c}(r,\varphi) \cong 0.815\Phi_{04} + 0.102\Phi_{10} \quad (6)$$

Ψ_{03} and $\Psi_{04,c}$ calculated by Eq. (6) are compared with numerical data in Table 3 where modal displacements based on Eq. (6) match the numerical data well. So, linear combinations in Eq. (6) approximate $\Psi_{04,c}$ and Ψ_{03} with reasonable accuracy and sound radiation due to modal vibration will be calculated based on these expressions.

Table 3 Vibration modes distorted by the radial slots

Mode Indices			Vibration Modes		Remarks
m	n	q	Analytical	Numerical	
0	3	-	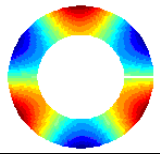	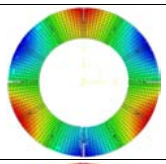	
0	4	c	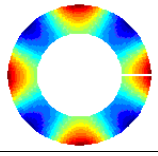	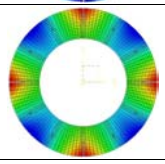	

2.2 Modal Sound Radiation

For a planar source, the far and free field sound pressure can be expressed as Eq. (6) based on the plane-wave approximation within the short-wavelength limits along with reference to Fig. 3.[14]

$$P(\mathrm{r}_p) = \frac{\rho_0 c_0 k}{2\pi} \int_{S_s} \frac{e^{ik|\mathrm{r}_p - \mathrm{r}_s|} \dot{W}(\mathrm{r}_s)}{|\mathrm{r}_p - \mathrm{r}_s|} \, dS \tag{7}$$

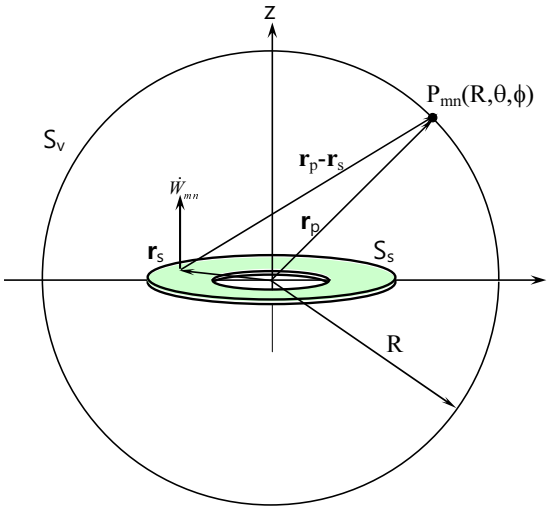

Fig. 3 Sound Radiation from the flexural vibration of a thin annular disc in spherical coordinate system

Here, ρ_0 is mass density of air, c_0 is sound speed and k is acoustic wave number. Sound pressure due to the (m, n)th flexural mode of a thin annular disk without any slot can be expressed as following equation within the shot-wavelength limit:[12-14]

$$P_{mn}(R,\theta,\phi) = \frac{\rho_0 c_0 k_{mn} e^{ik_{mn}R}}{R} \cos n\phi (-i)^{n+1} \mathrm{B}_n\left[\dot{w}(r)\right]$$
$$B_n\left[\dot{W}(r)\right] = \int_0^\infty \dot{W}(r) J_n(k_r r) r dr. \tag{8}$$

Here, $k_r = k_{mn}\sin\theta$, and $\dot{W}(r)$ is the variation of the surface velocity on the normal surfaces in the radial direction. Further, J_n is the Bessel function of order n.

If, as in the case of $\Psi_{02,q}$ and $\Psi_{04,s}$, global vibration modes are not seriously affected by the radial slots and can be reasonably approximated with Eq. (5), modal sound pressure due to the corresponding modes can be determined using following equation considering phase difference between the modes.

$$P_{mn,q}(R,\theta,\phi) = \frac{\rho_0 c_0 k_{mn,q} e^{ik_{mn,q}R}}{R} \cos n(\phi + \gamma_q) \, (-i)^{n+1} \mathrm{B}_n\left[\dot{w}(r)\right] \tag{9}$$

Here, γ_q is phase difference between two split modes which is 0 for q = c or $\pi/2n$ for q = s. With Eq. (9), sound pressures can be calculated at pre-determined observation points on the surface of the sphere of S_v that surrounds the disk and is centered at the disk center as shown in Fig. 3. The modal sound radiations, $\Lambda_{mn,c}$ and $\Lambda_{mn,s}$ for the two split (m, n)th modes can be determined from the sound pressure distribution over the surface of the sphere.[12]

On the other hand, if $\dot{w}(r)$ and global vibration modes are affected by the slots as in the case of Ψ_{03} and $\Psi_{04,c}$ with α = 0.45, sound pressure at a given receiver position should be modified accordingly. Since the acoustic system is assumed to be linear time-invariant, sound radiations due to Ψ_{03} and $\Psi_{04,c}$ that are linear combinations of Φ_{mn} can also be expressed as linear combinations of corresponding modal sound radiations(Γ_{mn}) as following equation.

$$\Lambda_{03}(r,\varphi) \cong 1.02\Gamma_{03} - 0.032\Gamma_{11}$$
$$\Lambda_{04,c}(r,\varphi) \cong 0.815\Gamma_{04} + 0.102\Gamma_{10} \tag{10}$$

Selected modal sound radiations ($\Lambda_{mn,q}$) calculated with Eq. (9) and (10) are compared with numerical data from finite element[14] and boundary element analyses[17] in Table 4 where two results match well each other.

Table 4 Selected modal sound radiation patterns for the sample disk with α = 0.45

Mode Indices			Modal Sound Radiation Pattern		Remarks
m	n	q	Analytical	Numerical	
0	2	c	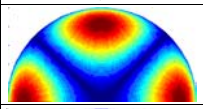	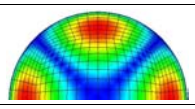	
0	2	s	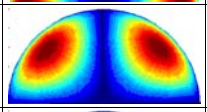	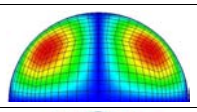	
0	4	c	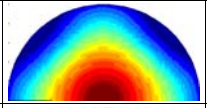	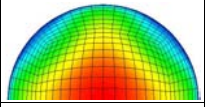	
0	4	s	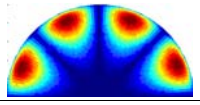	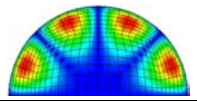	

In addition, from the far-field approximation, the modal sound powers $\Pi_{mn.c}$ and $\Pi_{mn.s}$ of (m, n)th mode is calculated using the following equation.

$$\Pi_{mn,q} = \left\langle I_{mn,q} S_V \right\rangle_s = \frac{R^2}{2\rho_0 c_0} \int_0^{2\pi} \int_0^{\pi} {P_{mn,q}}^2 \sin\theta \, d\theta \, d\phi \qquad (11)$$

Here, $I_{mn,q}$ are the acoustic intensity on the surface of S_v is the control surface where modal sound pressure is calculated.

3. Response to a Harmonic Force Fixed to the Disk

3.1 Modal Formulation

Modal response of annular disk with slots for a given harmonic excitation can be obtained using modal expansion technique. If the disk is excited by a multi-modal harmonic force at an arbitrary circular frequency ω and location $\mathbf{r}_f = (r_f, \varphi_f)$, several modes, including both split and repeated modes, are simultaneously excited. Based on the modal-expansion technique, velocity distribution (v) on the disk surfaces can be expressed in terms of modal velocity vectors of the disk as shown by the following equations.

$$\begin{aligned} \{v(\omega)\} &= \{\eta(\omega)\}^T \{\Psi^V\} \\ \{\Psi^V\} &= \{\Psi_1^V, \Psi_2^V, \Psi_3^V, \cdots, \Psi_l^V\} \end{aligned} \qquad (12)$$

In Eq. (12), Ψ^V is the velocity modal vector of the disk expressed as the modal displacement vector multiplied by the corresponding natural frequency (in rad/s) and η_l is the associated modal participation factor that can be expressed as follows:

$$\eta_l(\omega) = \frac{\Psi_l(r_f, \varphi_f)}{\omega_l^2 \left[1 - \omega^2/\omega_l^2 + i2\zeta_l(\omega/\omega_l)\right]} \qquad (13)$$

Here, ω_l and ζ_l are the natural frequency and modal damping ratio of mode l, respectively.

Earlier, Lee and Singh expressed the far-field sound pressure from thin or thick annular disks due to a multi-modal force excitation using the structural modal participation factors and modal sound pressures.[6,12] Applying the same procedure to the acoustic problem, the far-field pressure on a sphere (S_v) surrounding the thin disk given the surface velocity of Eq. (12) is expressed as:

$$\begin{aligned} P(\omega) &= \{\eta(\omega)\}^T \{\Lambda\} \ ; \\ \{\Lambda\} &= \{\Lambda_1, \Lambda_2, \Lambda_3, \cdots, \Lambda_l\} \ . \end{aligned} \qquad (14)$$

Here, Λ_l is the modal sound radiation for mode l.

Acoustic power spectra, Π(ω) of the disk due to an arbitrary harmonic excitation f(t) is also obtained from the far-field sound pressures on a sphere surrounding the disk as:

$$\Pi(\omega) = \frac{1}{2} \int_0^{2\pi} \int_0^{\pi} \frac{P^H(\omega) P(\omega)}{\rho_0 c_0} R^2 \sin\theta \, d\theta \, d\phi \qquad (15)$$

3.2 Steady State Response of a Pair of Split Modes

3.2.1 Effects of Excitation Location

If global vibration modes can be reasonably approximated with Eq. (5), $\Psi_{mn,q}(r_f, \varphi_f)$ in Eq. (13) can be expressed as follows considering vibration shapes of two modes given in Eq. (5) and the assumptions in Section 1.

$$\begin{aligned} \Psi_{mn,c}(r_f, \varphi_f) &= W(r_f) \cos n\varphi_f \\ \Psi_{mn,s}(r_f, \varphi_f) &= W(r_f) \sin n\varphi_f \end{aligned} \qquad (16)$$

Consequently, contributions of two split modes on surface velocity and sound pressure due to a harmonic excitation at $\boldsymbol{r}_f$ with circular frequency ω can be expressed as following equations.

$$v(\omega) \cong \frac{\Psi_{mn,c} W(r_f) \cos n\varphi_f}{\omega_{mn,c}^2 - \omega^2 + i2\zeta_{mn,c}\omega\omega_{mn,c}} + \frac{\Psi_{mn,s} W(r_f) \sin n\varphi_f}{\omega_{mn,s}^2 - \omega^2 + i2\zeta_{mn,s}\omega\omega_{mn,s}} \qquad (17)$$

$$P(\omega) \cong \frac{\Gamma_{mn,c} W(r_f) \cos n\varphi_f}{\omega_{mn,c}^2 - \omega^2 + i2\zeta_{mn,c}\omega\omega_{mn,c}} + \frac{\Gamma_{mn,s} W(r_f) \sin n\varphi_f}{\omega_{mn,s}^2 - \omega^2 + i2\zeta_{mn,s}\omega\omega_{mn,s}} \qquad (18)$$

As one can see from Eq. (17) and (18), surface velocity and sound radiation for the given excitation are significantly affected by the location of excitation. For instance, $\Psi_{mn,c}$ does not contribute to total sound radiation when $\varphi_f = 0$ or $\varphi_f = \pi/2$ for the example case given in Fig. 1 and Table 1.

On the other hand, as in the case of $\Psi_{04,c}$ and Ψ_{03} given $\alpha = 0.45$, if the global vibration modes are severely affected by the slots and should be expressed as Eq. (6), modal participation factors for two split modes should be expressed as follows:

$$\eta_{mn,q}(\omega) = \frac{\sum A_{mn} \Phi_{mn}(r_f, \varphi_f)}{\omega_{mn,q}^2 \left[1 - \omega^2/\omega_{mn,q}^2 + i2\zeta_{mn,q}(\omega/\omega_{mn,q})\right]} \qquad (19)$$

Corresponding contributions from the mode on surface velocity and sound pressure due to the harmonic excitation can be expressed as following equations.

$$v(\omega) \cong \frac{\Psi_{mn,q} \sum A_{mn} \Phi_{mn}(r_f, \varphi_f)}{\omega_{mn,q}^2 - \omega^2 + i2\zeta_{mn,q}\omega\omega_{mn,q}} \qquad (20)$$

$$P(\omega) \cong \frac{\Lambda_{mn,q} \sum A_{mn} \Phi_{mn}(r_f, \varphi_f)}{\omega_{mn,q}^2 - \omega^2 + i2\zeta_{mn,q}\omega\omega_{mn,q}} \qquad (21)$$

3.2.2 Sound powers from self and mutual radiation terms

If several structural modes are simultaneously excited, the total sound power Π of Eq. (15) at frequency ω can be decomposed into two groups: a. Π from the self-radiation of individual modes, and b. Π from the mutual radiation between any two (or more) structural modes. For the case of a uniform annular disk case, Eq. (15) suggests that coupling could exist between any two (m, n) modes. Thus, define the sound power generated by the coupling between the (m_i n_i, q_i) mode and (m_j n_j, q_j) mode as:[13]

$$\Pi_{m_i n_i q_i}^{m_j n_j q_j} = \frac{R^2}{2\rho_0 c_0} \int_0^{2\pi} \int_0^{\pi/2} P_{m_i n_i q_i} P^*_{m_j n_j q_j} \sin\theta d\theta d\phi \qquad (22)$$

Here, $\Pi_{m_i n_i q_i}^{m_j n_j q_j}$ is the power from self radiation when $m_i = m_j$, $n_i = n_j$ and $q_i = q_j$. Otherwise $\Pi_{m_i n_i q_i}^{m_j n_j q_j}$ is due to the mutual radiation between (m_i, n_i q_i) and (m_j, n_j q_j) modes. By repeating the procedure given above, radiated powers associated with individual modes of the disk can be obtained along with sound powers due to the coupling effects between any two structural modes.

Further, the total acoustic power due to multi-modal excitation could be obtained in terms of a linear combination of the sound

powers from self and mutual-radiation terms as follows:

$$\Pi(\omega) = \sum\sum \eta_{m_i n_i q_i}(\omega)\ \eta_{m_j n_j q_j}(\omega)\ \Pi^{m_j n_j q_j}_{m_i n_i q_j} \qquad (23)$$

The sound powers Π(ω) for the case of a unit harmonic force are calculated using Eq. (23) and compared in Fig. 4 with those with Eq. (15). The calculations based on the self and mutual radiation powers match well with the modal expansion technique. Therefore, one may easily calculate acoustic power for any arbitrary force using Eq. (22). Also, as one can see in the figure, at the contribution from $\Psi_{04,s}$ to the total acoustic power is very small compare to that from $\Psi_{04,c}$.

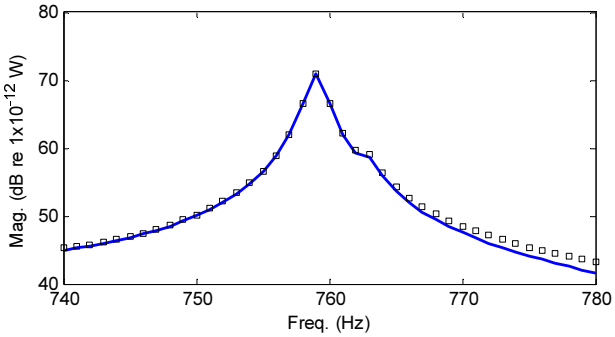

Fig. 4 Π/f(ω)of the sample disk with α = 0.45 for $\mathbf{r}_f$ = (0.139, π/6). Key: ——, By Eq. (15); ▫ ▫ ▫, By Eq. (23)

3.3 Validation Studies

Analytical solutions and numerical results are confirmed with experimental results for the sample case given in Fig. 1 and Table 1. Only the first 9 modes are considered in this verification procedure since the relevant upper frequency for acoustic radiation study is 0.8 kHz.

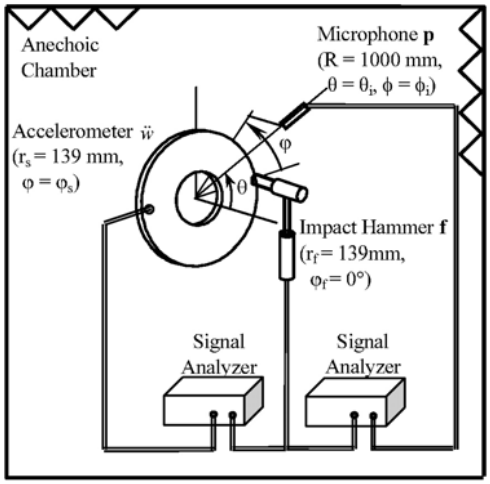

Fig. 5 Vibro-acoustic experiment setup for the validation study

In modal experiments, the excitation force f(t) is applied in the normal direction by an impulse hammer at φ = φ_f at the outer edge of the disk as explained in Fig. 5. The resolution (Δf) of this experiment is set to be 1.0 Hz. Accelerance spectra, $\ddot{w}$ /f(ω) for the sample disk with α = 0.45 and uniform disk are obtained using experimental setup given in Fig. 5 and natural frequencies ($\omega_{mn,q}$) and modal damping ratios ($\zeta_{mn,q}$) are extracted from $\ddot{w}$ /f(ω). Numerical and analytical mobility spectra $\dot{w}$ /f(ω) for the sample disks are also calculated using Eq. (11) from analytical or numerical eigensolutions along with modal damping ratio from the experiments. Spectra at specific receiver locations $\mathbf{r}_s$ = (0.139, π/4) and $\mathbf{r}_s$ = (0.139, π/8) for a harmonic excitation at $\mathbf{r}_f$ = (0.139, π/6) are obtained using three approaches and compared each other in Fig. 6. As shown in the figure, three results match well in the vicinities of the peaks though some discrepancies are being found in the off-resonant regions. So, it could be concluded that total procedure introduces above has reasonable accuracy in calculating structural responses of the disk for a given harmonic excitation. Also, note that contributions from $\Psi_{04,c}$ and $\Psi_{04,s}$ to the total vibration of the disk for the excitation at $\mathbf{r}_f$ = (0.139, π/6) are almost same. But, as shown in Fig. 4, acoustic power from $\Psi_{04,c}$ is much bigger than that from $\Psi_{04,s}$. So, it can be inferred that $\Psi_{04,c}$ is much more efficient in sound radiation than $\Psi_{04,s}$.

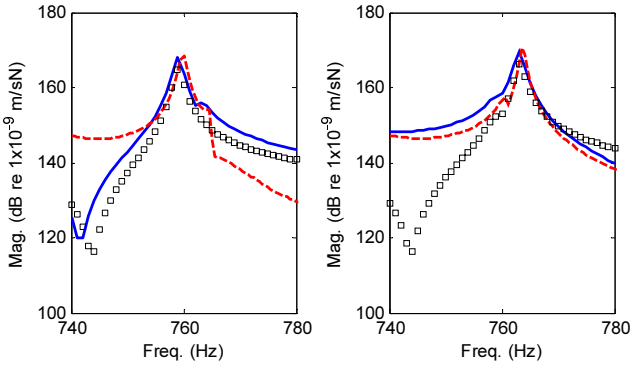

Fig. 6 $\dot{w}$ /f(ω) of the sample disk with α = 0.45 for $\mathbf{r}_f$ = (0.139, π/6). (a) $\mathbf{r}_s$ = (0.139, π/4) (b) $\mathbf{r}_s$ = (0.139, π/8). Key: ▫ ▫ ▫, Numerical; ——, Analytical; - - -, Experiments

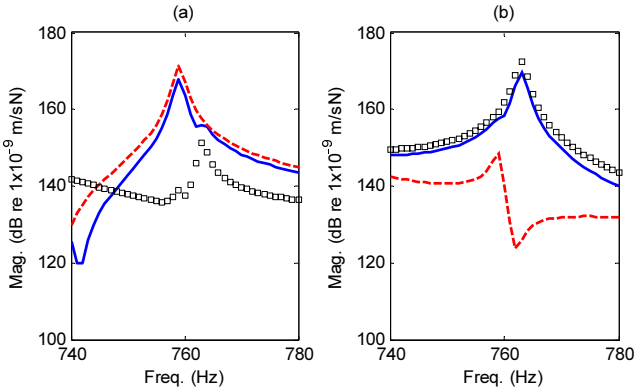

Fig. 7 $\dot{w}$ /f(ω) of the sample disk with α = 0.45. (a) $\mathbf{r}_s$ = (0.139, π/4) (b) $\mathbf{r}_s$ = (0.139, π/8). Key: ▫ ▫ ▫, $\mathbf{r}_f$ = (0.139, π/8); ——, $\mathbf{r}_f$ = (0.139, π/6); - - -, $\mathbf{r}_f$ = (0.139, π/4)

The effects of excitation locations on the mobility spectra are studied using the analytical procedure introduced in Section 3.2.1. $\dot{w}$ /f(ω) at two receiver positions used above for a unit harmonic excitation at three excitation locations, $\mathbf{r}_f$ = (0.139, π/8), $\mathbf{r}_f$ = (0.139, π/6) and $\mathbf{r}_f$ = (0.139, π/4) calculated using Eq. (12) and (13) are given in Fig. 7 where the effects are clearly shown. So it is expected

that total surface vibration in the disk will be affected by the location of excitation.

Acoustic frequency response functions, p/f(ω), for the sample disk with $\alpha = 0.45$ are also calculated from analytical and numerical $\Lambda_{mn,q}$ along with experimental $\zeta_{mn,q}$ with Eq. (19) or (21). The results for selected receiver position $\mathbf{r}_p = (1, 0, 0)$ and excitation location $\mathbf{r}_f = (0.139, \pi/6)$ are compared with experimental data in Fig. 8. As one can see in the figure, the results from three approaches show good agreements verifying the accuracy of the procedure given above.

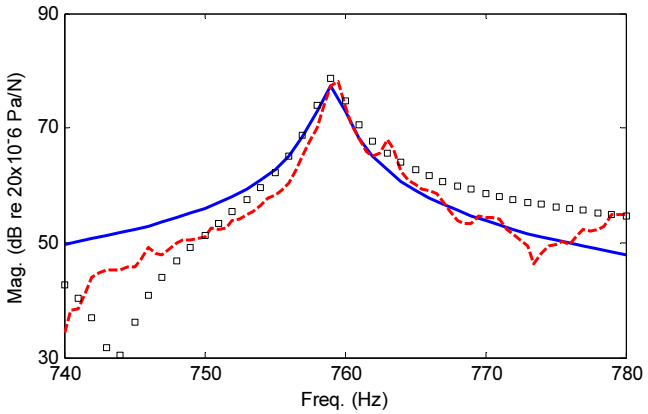

Fig. 8 p/f(ω) of the sample disk with $\alpha = 0.45$ at $\mathbf{r}_p = (1, 0, 0)$ for $\mathbf{r}_f = (0.139, \pi/6)$. Key: ▫ ▫ ▫, Numerical; ——, Analytical; - - -, Experiment

Acoustic frequency response function at a receiver positions used above for the unit harmonic excitation at three excitation locations, $\mathbf{r}_f = (0.139, \pi/8)$, $\mathbf{r}_f = (0.139, \pi/6)$ and $\mathbf{r}_f = (0.139, \pi/4)$ calculated using Eq. (22) are compared each other in Fig.9. As shown in the figure, sound pressure at a given receiver position is severely affected by the location of excitation.

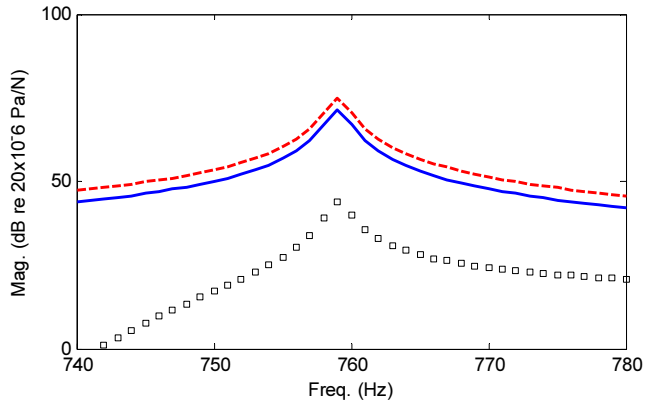

Fig. 9 p/f(ω) of the sample disk with $\alpha = 0.45$. Key: ▫ ▫ ▫, $\mathbf{r}_f = (0.139, \pi/8)$; ——, $\mathbf{r}_f = (0.139, \pi/6)$; - - -, $\mathbf{r}_f = (0.139, \pi/4)$

4. Conclusions

This article has examined the effects of narrow radial slots on the vibro-acoustic characteristics of thin annular disks. Pre-developed analytical solution for eigensolutions of thin annular disk with radial slots has been checked numerically and experimentally. According to the results, when the length of slots exceeds a certain limit, the global vibration modes are affected by the slots and natural frequencies from analytical solution would include some errors.

Modified vibration modes are expressed as linear combinations of modal vibrations of a corresponding uniform disk. Also, modal sound radiations from the modified vibration modes are expressed as the linear combinations of modal sound radiation of the uniform disk that are defined with pre-developed analytical solution. The results are verified with numerical data for selected modes showing that the procedure introduced here has reasonable accuracy in predicting sound radiation from the modal vibrations of disks with slots. Also, acoustic powers for the two split modes with same m and n could be calculated based on the modal sound radiations.

Structural and acoustic responses of the disks for an arbitrary harmonic excitation are obtained from pre-defined modal vibration and modal sound radiation using modal expansion technique. Verification on the acoustic frequency response function at a specific receiver position and acoustic power spectra for a given excitation confirm the accuracy of the procedure.

The procedure introduced in this article can be efficiently used to calculate modal and multi-modal sound radiations from thin annular disks containing narrow radial slots with reasonable accuracy. Also, the existence of asymmetries such as slots or holes can be detected by examining the acoustic radiation characteristics such as p/f(ω) or Π(ω) at a specific position.

In a future study, this procedure will simultaneously consider both out-of-plane and in-plane components of the disc vibration. Modal interaction effects and sound radiation from coupled modes will also be studied.

REFERENCES

1. Mote, C. D. Jr., "Stability Control Analysis of Rotating Plates by Finite Element: Emphasis on Slots and Holes," Journal of Dynamic Systems, Measurement, and Control, March, Vol. 94, No. 1, pp. 64-70, 1972.

2. Yu, R. C. and Mote, C. D. Jr., "Vibration and Parametric Excitation in Asymmetric Circular Plates under Moving Load," Journal of Sound and Vibration, Vol. 119, No. 3, pp. 409-427, 1987.

3. Honda, Y., Matsuhisa, H. and Sato, S., "Modal Response of a Disk to A Moving Concentrated Harmonic Force," Journal of Sound and Vibration, Vol. 102, No. 4, pp. 457-472, 1985.

4. Shen, I. Y. and Mote, C. D. Jr., "Dynamic Analysis of Finite Linear Elastic Solids Containing Small Elastic Imperfections: Theory with Application to Asymmetric Circular Plates," Journal of Sound and Vibration, Vol. 155, No. 3, pp. 443-465, 1992.

5. Rim, K. H. and Mote, C. D. Jr., "Unstable Phenomenon for High-Speed Rotating Circular Saws," Transactions of the Korean Society for Noise and Vibration Engineering, Vol. 9, No. 6, pp. 1210-1217, 1999.

6. Lee, H. I., "Modal Vibration Characteristics of an Annular Disk Containing Evenly Spaced Narrow Radial Slots," Transactions of the Korean Society for Noise and Vibration Engineering, Vol. 19, No. 6, pp. 560-568, 2009.

7. Thompson, W. Jr., "The computation of self- and mutual-radiation impedances for annular and elliptical pistons using Bouwkamp integral," Journal of Sound and Vibration, Vol. 17, No. 2, pp. 221-233, 1971.

8. Lee, M. R. and Singh, R., "Analytical formulations for annular disk sound radiation using structural modes." Journal of the Acoustical Society of America, Vol. 95, No. 6, pp. 3311-3323, 1994.

9. Levine, H. and Leppington, F. G., "A note on the acoustic power output of a circular plate," Journal of Sound and Vibration, Vol. 121, No. 5, pp. 269-275, 1988.

10. Rdzanek, W. P. Jr. and Engel, Z., "Asymptotic formula for the acoustic power output of a clamped annular plate," Applied Acoustics, Vol. 60, No. 5, pp. 29-43, 2000.

11. Wodtke, H. W. and Lamancusa, J. S., "Sound power minimization of circular plates through damping layer placement," Journal of Sound and Vibration, Vol. 215, No. 5, pp. 1145-1163, 1998.

12. Lee, H. and Singh, R., "Acoustic radiation from out-of-plane modes of an annular disk using thin and thick plate theories," Journal of Sound and Vibration, Vol. 282, No. 1-2, pp. 313-339, 2005.

13. Lee, H. and Singh, R., "Self and mutual radiation from flexural and radial modes of a thick annular disk," Journal of Sound and Vibration, Vol. 286, No. 4-5, pp. 1032-1040, 2005.

14. Junger, M. C. and Feit, D., "Sound, Structures, and Their Interactions," MIT Press, pp. 88-90, 1985.

15. Kim, I. S. and Kim, Y. S., "Active Vibration Control of Trim Panel Using a Hybrid Controller to Regulate Sound Transmission," Int. J. Precis. Eng. Manuf., Vol. 10, No. 1, pp. 41-47, 2009.

16. UGS Corp., "I-DEAS User's manual Version 11," 2006.

17. NIT, "SYSNOISE User's manual Revision 5.6," 2005.